Microstructures and toughening mechanisms of organoclay/polyethersulphone/epoxy hybrid nanocomposites

Yang Wang*, Boming Zhang, Jinrui Ye

Department of Polymer and Composite Materials, Beihang University, Beijing 100191, China

ABSTRACT

Hybrid nanocomposites (HNCs) with high fracture toughness were successfully prepared by incorporating polyethersulphone (PES) and organoclay into epoxy resin. Their microstructures were studied. They were composed of homogeneous PES/epoxy matrices and micron-scale organoclay agglomerates. These agglomerates consisted of smaller tactoid-like regions which were comprised of ordered exfoliated nanolayers. The toughening mechanisms of the two tougheners were also studied and then related to their microstructures. For one thing, the PES which was dissolved in the epoxy resin homogeneously improved the ductility of the epoxy resin and made it easier to deform. For another, the organoclay agglomerates induced crack front bowing, crack bridging, crack deflection, crack bifurcation and plastic deformation of the matrices on the micron-scale, respectively. These toughening processes were achieved by the ordered exfoliated nanolayers with various orientations, which debonded from the matrices, bridged the cracks and induced the plastic deformation of the matrices on the nanoscale.

© 2011 Elsevier B.V. All rights reserved.

1. Introduction

As the matrices of fiber-reinforced composites, epoxy resins were often toughened by a secondary phase [1]. Since 1980s, significant progress has been made in improving their fracture toughness with inorganic particle [2], liquid rubber [3], thermoplastic [4,5], etc.

With the development of nanotechnology, the incorporation of nanoparticles such as nanoclay was regarded as an effective way to toughen epoxy resins [6,7]. The nanoclay could improve their fracture toughness without leading to a dramatic decrease in other desirable mechanical properties such as modulus or strength. However, its dispersion and morphology could markedly affect the mechanical properties of the synthesized nanocomposites [8].

In recent years, to incorporate two tougheners into epoxy resins simultaneously has been deemed to be a better strategy for getting a further improvement in their mechanical properties, particularly in their fracture toughness. As one of the promising components in these ternary hybrid nanocomposites (HNCs), nanoclay is playing an increasingly significant role in toughening epoxy resins [9–11].

With the widespread use of various tougheners, their toughening mechanisms were also studied. Crack deflection, crack front bowing (including crack pinning), crack tip bifurcating (i.e., branching), microcracking, crack tip blunting, crack bridging and micro-shear banding are the well-known toughening mechanisms which have been applied to various polymer systems up to now [6,12–17]. A variety of single-toughener systems have been researched and each toughener usually has more than one toughening mechanism, while the toughening mechanisms of two-toughener systems are more complicated and the synergistic toughening effect of the two tougheners is hard to attain. Accordingly, further research should be done on the two-toughener systems to reveal the complicated mechanisms for getting better mechanical properties.

In this study, our objective is to prepare organoclay-reinforced PES-modified epoxy-based hybrid nanocomposites (i.e., organoclay/PES/epoxy HNCs) with high fracture toughness, reveal the microstructures of the two tougheners in them and dig out their toughening mechanisms.

2. Experimental

2.1. Preparation of samples

In order to prepare the HNCs, PES (5 wt%, Sumitomo Corporation) and epoxy oligomer (DER331®, Dow Chemical Company) were completely dissolved in methylene chloride (Tianjin Kermel Chemical Reagent Co., Ltd.) at room temperature. Then organoclay (1 wt% or 3 wt%, I.30E, Nanocor) was dispersed in the solution with vigorous mechanical stir and the mixture was sonicated for at least 30 min. The translucent mixture was then placed into a water bath and a hot vacuum oven to drive off the solvent. In the next stage,

---

the stoichiometric amount of the hot DDS (SUZHOU YINSHENG Chemical Co., Ltd.) was added to the mixture with a fierce stir. Subsequently, the mixture was cast into a preheated mould treated with a release agent (Frekote 44-NC, Loctite Corporation). At last, the mould was cured at 120 °C for 24 h and subsequently post-cured at 180 °C for additional 2 h.

This preparing method was also used to synthesize the nanocomposites, the PES/epoxy blend and the neat cured epoxy resin by omitting the incorporation of PES, organoclay and both of them, respectively. The same curing schedule was applied.

2.2. Physical measurement

Dynamic mechanical properties of all the samples were measured by a DMA Q800 analyzer produced by TA Instruments Corporation at a fixed frequency of 1 Hz and a heating rate of 3 °C/min. The tests were conducted under dual cantilever mode for the samples of size 60 mm × 6 mm × 3 mm.

X-ray diffraction (XRD) measurements were performed on a D/max-γB diffractometer with a Cu Kα radiation (λ = 0.154 nm) produced by Rigaku Corporation. The acceleration voltage and acceleration current were 40 kV and 20 mA, respectively. The scanning speed and the step length were 0.6° min^{-1} and 0.006°, respectively. The 2θ ranged from 0.6° to 10°.

For scanning electron microscope (SEM) observation, all the fractured specimens were coated with a layer of gold around 200 Å thick and observed by a scanning electron microscope (Philips XL-30).

A JOEL JEM-2100F transmission electron microscope (TEM) was used at an accelerating voltage of 200 kV to observe the microtomed thin-section specimens of 50–60 nm thickness. Before the observation, the samples were first fractured according to the double-notched four-point bending (DN-4PB) test [18]. The subcritical crack tip damage zones were then carefully polished, trimmed and microtomed for being observed on 200 mesh copper grids.

2.3. Mechanical properties

The fracture toughness of all the cured resins was measured from the critical stress intensity factor (K_{IC}) in the single-edge notched three-point bending (SEN-3PB) test according to ASTM D5045-99. The dimensions of each sample were 70 mm (L) × 10 mm (W) × 5 mm (B) and the span was 40 mm (S). A screw-driven Instron machine (Instron 5569) was used at a crosshead speed of 0.5 mm/min. At least 5 specimens of each composition were tested.

3. Results and discussions

3.1. Microstructures of PES and organoclay in the HNCs

In this study, 5 wt% PES was added to the epoxy resins for preparing the organoclay/PES/epoxy HNCs and the PES/epoxy blend. DMTA was then used to observe the phase morphologies in them. As shown in Fig. 1, all the curves have single peaks, which is the characteristic of homogeneous phase morphology. It demonstrates that the PES was dissolved in the epoxy resins homogeneously and phase decomposition between them was suppressed greatly.

The morphology of the dispersed organoclay in the nanocomposites and the HNCs was investigated with XRD (Fig. 2) and TEM (Fig. 3). It can be seen from Fig. 2 that there are no peaks in the XRD curves, which indicates that the organoclay was all exfoliated. Since 2θ is ranging from 0.6° to 10°, the d-spacing of the dispersed organoclay is all larger than 12 nm in accordance with the Bragg's relation [7]. Fig. 3 shows that the organoclay possesses mainly ordered exfoliated structure in the HNCs and the d-spacing is more than 12 nm.
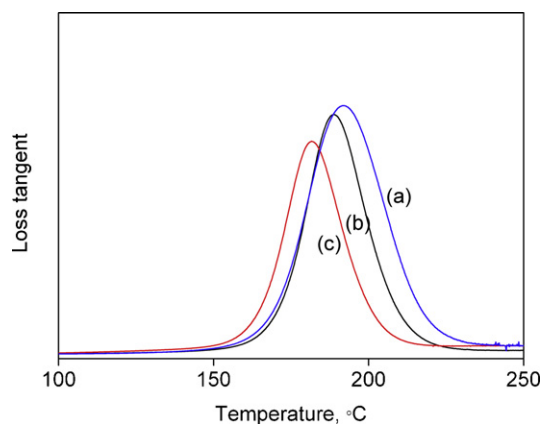

Fig. 1. DMTA curves of Loss tangent vs. temperature for three samples: (a) the PES/epoxy blend; (b) the organoclay (1 wt%)/PES/epoxy HNC; (c) the organoclay (3 wt%)/PES/epoxy HNC.

The TEM images of the organoclay in the nanocomposites which are not demonstrated here show similar patterns. It should be noted that the organoclay was still close to each other to form various micron-scale agglomerates (Fig. 3(c)). These agglomerates with loose structure inside are commonly composed of many smaller tactoid-like regions ca. 1 μm in diameter with ordered exfoliated nanolayers parallel to each other. Since there are no electrostatic attractive force and van der Waals force between the nanolayers whose d-spacing exceeds 8 nm [7], these tactoid-like regions are easy to be fractured and separated from each other by the external stress. Particularly, the tactoid-like regions have various orientations which are predicted to influence the fracture behaviour and thus the fracture toughness of the HNCs. In this study, the orientation of an organoclay nanolayer is defined as the direction its end surface faces and the orientation of a tactoid-like region is regarded as the orientation of most of its nanolayers.

3.2. Toughening mechanisms of the HNCs

Table 1 presents the Model-I fracture toughness values (K_{IC}) of the prepared neat cured epoxy resin, PES/epoxy blend, nanocomposites and HNCs. It shows that the K_{IC} values of the HNCs are the highest two and therefore the PES and the organoclay have a marked synergistic toughening effect on the epoxy resin. Since phase decomposition was greatly suppressed in the HNCs, the toughening mechanisms mainly relate to the ductility of the
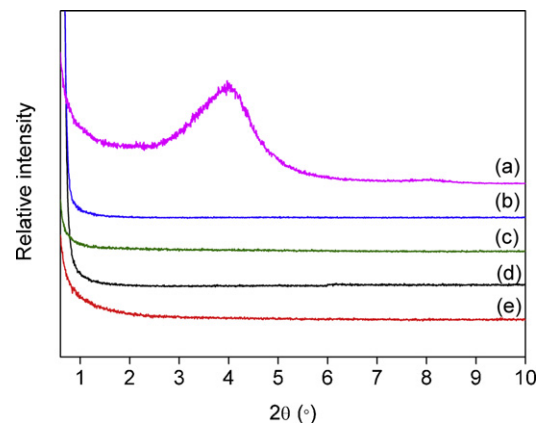

Fig. 2. XRD patterns of the specimens: (a) the organoclay; (b) the organoclay (1 wt%)/epoxy nanocomposite; (c) the organoclay (3 wt%)/epoxy nanocomposite; (d) the organoclay (1 wt%)/PES/epoxy HNC; (e) the organoclay (3 wt%)/PES/epoxy HNC.
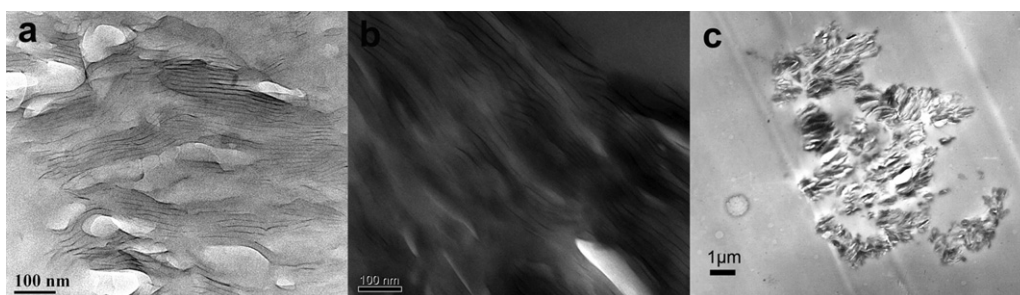
Fig. 3. TEM images of the morphologies of the organoclay in the HNCs: (a) large organoclay agglomerate in the HNC with 1 wt% organoclay; (b) large organoclay agglomerate in the HNC with 3 wt% organoclay; (c) organoclay agglomerate ca. 10 μm in diameter in the HNC with 3 wt% organoclay.

homogeneous PES/epoxy matrices [15] and the functions of the organoclay [6].

SEM micrographs in Fig. 4 demonstrate that the river-markings (described by Liu [8]) and characteristic tail structures (presented by Lange [12]) around the organoclay micron-scale agglomerates are much deeper in the PES-modified sample (Fig. 4(a)) compared with those in the control without the PES (Fig. 4(b)). The result proves that the incorporation of PES markedly enhanced the ductility, i.e., toughenability, of the epoxy matrices.

For researching the influence of the organoclay on the fracture toughness of the HNCs, the micro-mechanical deformations were studied using SEM. Fig. 5(a) shows that characteristic tail structures formed behind the globular organoclay agglomerates in the process zone. When the organoclay content increased to 3 wt%, the fracture surface became rougher and more characteristic tails appeared and interconnected with each other (Fig. 5(b)). Since the characteristic tail structure usually forms when the two secondary crack fronts separated by a particle meet with each other after crack front bowing, crack front bowing is a toughening mechanism of the organoclay agglomerates.

In Fig. 6(a) and (b), two halves of the fractured organoclay agglomerate ca. 30 μm in diameter and ca. 10 μm in diameter are observed in the HNC with 1 wt% organoclay. The white regions inside and around them clearly show that plastic deformation took place after the crack front passed them. Since it is obvious that the organoclay agglomerates acted as bridges between the two fracture surfaces, the crack bridging accompanied by the plastic deformation of the matrices is also a toughening mechanism of the organoclay agglomerates.

Furthermore, the fracture position of the agglomerate ca. 10 μm in diameter on the right side of Fig. 6(a) is higher than that of the agglomerate ca. 30 μm in diameter adjacent to it. In higher organoclay content system, the quantity of large agglomerates whose diameters are larger than 30 μm markedly increased, which led to the formation of the more complicated fracture surfaces (Fig. 6(c) and (d)). Besides, the various fracture positions inside one agglomerate can also be observed in Fig. 6(e). The river-markings which formed around the fractured agglomerates outlined the jagged surfaces and showed that crack deflection took place. Therefore, crack deflection induced by the various fracture positions of the organoclay agglomerates is another toughening mechanism of the organoclay agglomerates.

In Fig. 7, debonding of the organoclay agglomerates ca. 30 μm in diameter from the matrix is clearly seen. In addition, the white regions around the agglomerates indicate that the debonding process was accompanied by the plastic deformation of the matrix. Since the epoxy oligomers were easier to diffuse into the organoclay interlayers than the macromolecular chains of the PES were, the agglomerates mainly consisted of the cured epoxy resin and the organoclay. Therefore, their components were quite different from those of the PES/epoxy matrices. This difference led to the thermal residual misfit between the agglomerates and their matrices and therefore facilitated the debonding process. It should be noted that this debonding process led to the formation of the crack branches along the agglomerate/matrix interface normal to the direction of crack propagation. As a result, crack bifurcation accompanied by the plastic deformation of the matrices is a toughening mechanism of organoclay agglomerates too.

In order to further reveal the role of the ordered exfoliated nanolayers, TEM was used to observe the interior of these agglomerates in the thin-section DN-4PB samples with sub-critical cracks. Fig. 8 shows part of the DN-4PB damage zone of the HNC with 1 wt% organoclay. It is obvious that debonding and bridging are the main effects of the nanolayers. The unfractured and fractured nanolayers show their bridging effect in the magnified image of Fig. 8(a) and (c), respectively. Since the nanolayers perpendicular to the direction of the crack propagation (Fig. 8(a)) are more effective in producing the crack branches than the nanolayers parallel to the direction of the crack propagation (Fig. 8(b)), the orientations of the tactoid-like regions composed of these nanolayers are predicted to have significant influence on the formation of the crack branches. According to the research of microcracking in the fiber-reinforced composites laminates, the microcracks would terminate when the interface between the 0 and 90° ply groups was reached and then would bifurcate at 0°/90° interface to form the delamination which would subsequently propagate along the fiber/matrix interface [19]. It seems that the function of the organoclay tactoid-like regions is very like that of the fiber ply groups. The tactoid-like regions whose orientations are not perpendicular to the direction of the crack propagation are expected to enable the main crack to bifurcate and therefore form the crack branches. Since the main crack usually propagate along these crack branches, crack deflection will then form after the crack bifurcation. In some cases, some crack branches can be terminated in the tactoid-like regions at

Table 1
Fracture toughness of the neat cured epoxy resin, the PES/epoxy blend, the nanocomposites and the HNCs (K_{IC} stands for the critical value of Mode-I fracture toughness).

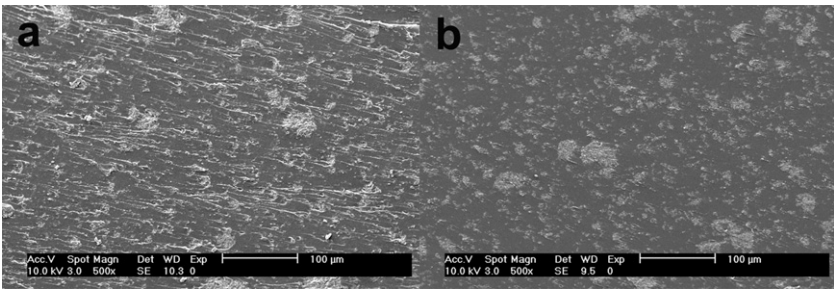| Specimens	Neat epoxy	Organoclay (1 wt%)/epoxy	Organoclay (3 wt%)/epoxy
K_{IC} (MPa m$^{1/2}$)	0.58 ± 0.11	0.73 ± 0.10	0.81 ± 0.08
Specimens	PES/epoxy	Organoclay (1 wt%)/PES/epoxy	Organoclay (3 wt%)/PES/epoxy
K_{IC} (MPa m$^{1/2}$)	0.77 ± 0.10	1.15 ± 0.14	0.95 ± 0.07

Fig. 4. SEM micrographs of the fracture surfaces of the organoclay-filled samples after SEN-3PB test: (a) organoclay (1 wt%)/PES/epoxy HNC; (b) organoclay (1 wt)%/epoxy nanocomposite.
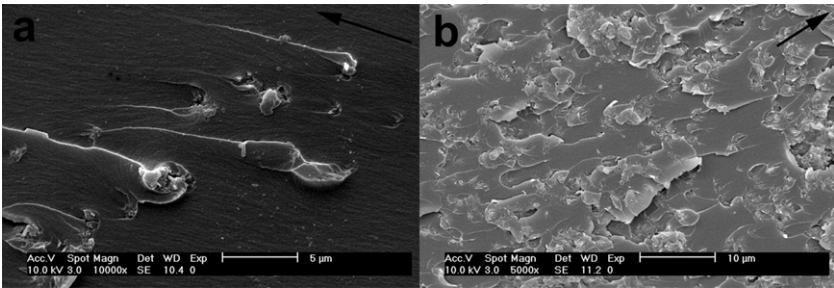

Fig. 5. SEM images of the fracture surfaces of the HNCs: (a) the characteristic tail structures on the fracture surface of the HNC with 1 wt% organoclay; (b) characteristic tail structures on the rough fracture surface of the HNC with 3 wt% organoclay. The arrows in the images indicate the direction of crack propagation.
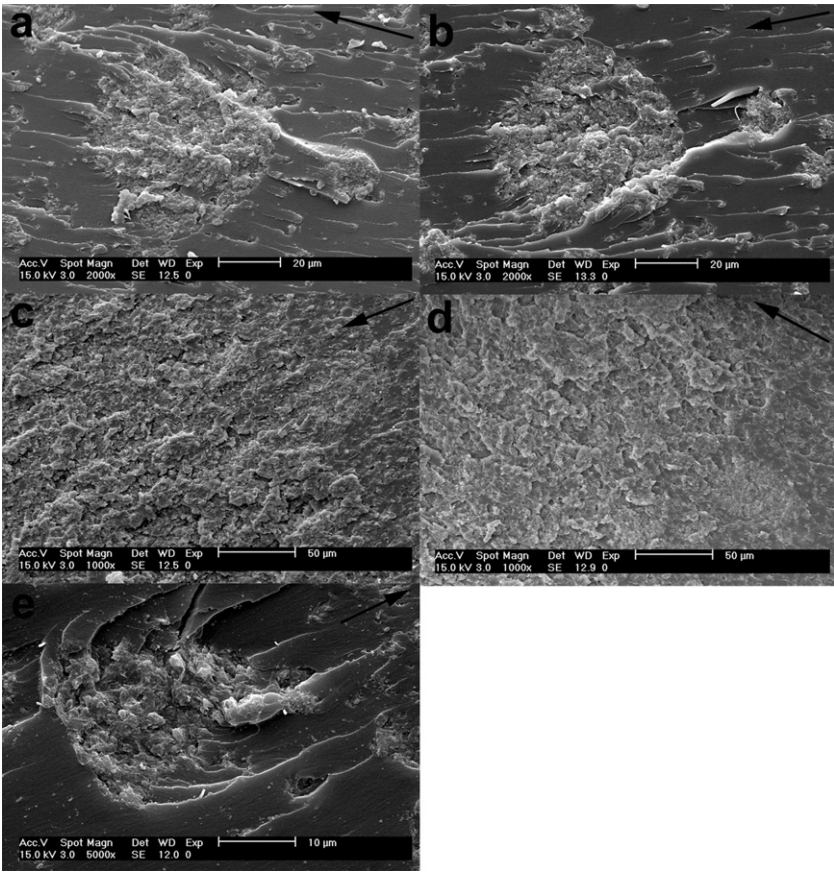

Fig. 6. SEM micrographs of the fracture surfaces of the HNCs after SEN-3PB test: (a) a region on the fracture surface of the HNC with 1 wt% organoclay; (b) the corresponding region on the symmetrical fracture surface of (a); (c) a region on the fracture surface of the HNC with 3 wt% organoclay; (d) the corresponding region on the symmetrical fracture surface of (c); (e) the various fracture positions inside one agglomerate on the fracture surface of the HNC with 1 wt% organoclay. The arrows in the images indicate the direction of crack propagation.
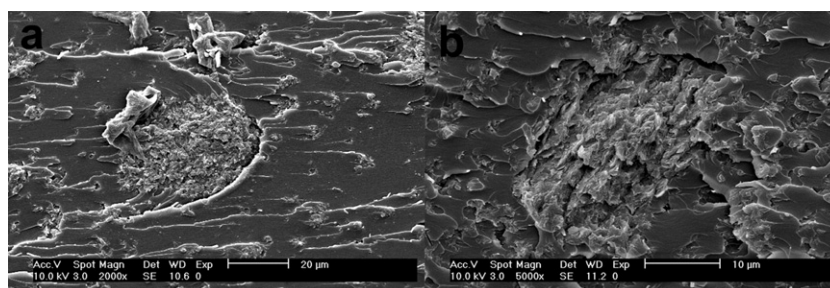
Fig. 7. SEM images of the fracture surfaces of SEN-3PB samples: (a) partial debonding of the organoclay agglomerate in the HNC with 1 wt% organoclay; (b) partial debonding of the organoclay agglomerate in the HNC with 3 wt% organoclay.
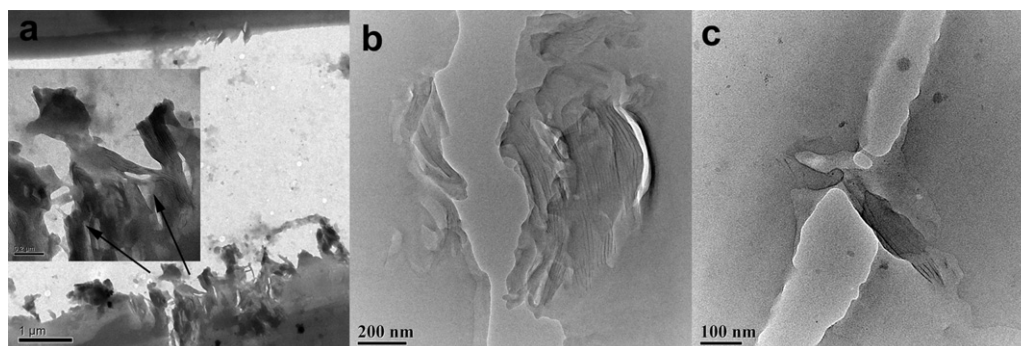

Fig. 8. TEM micrographs of DN-4PB damage zones of the HNC with 1 wt% organoclay: (a) fractured organoclay agglomerates in part of the damage zone of the sub-critical crack; (b) debonding of organoclay nanolayers along the direction of the crack propagation; (c) bridging effect of the unfractured organoclay nanolayers.

very early stage by the bridging effect of the nanolayers and plastic deformation of the matrices. In consequence, only the crack deflection can be observed around these tactoid-like regions. Most of the observed energy dissipation mechanisms of the nanolayers are illustrated in Fig. 9. From right to left, the crack bifurcation, the bridging effect of the unfractured nanolayers, the bridging effect of the fractured nanolayers, the debonding of the nanolayers from the matrix and the crack deflection without crack branches can be definitely seen in the scheme. It is presumed that the tactoid-like regions with various orientations will lead to the crack bifurcation and crack deflection.

To prove that the scheme in Fig. 9 works, the DN-4PB thin-section sample with more integrated sub-critical crack was further observed on a copper grid under TEM. The front part of the sub-critical crack and the close-ups of its four consecutive parts are shown in Fig. 10. The crack was partially covered by the copper grid. The main crack propagated in the matrix (Fig. 10(d)) and then bifurcated when it met with the organoclay agglomerate ca. 7 μm

Fig. 9. Scheme of most of the energy dissipation mechanisms which have been observed in Fig. 8 in the organoclay agglomerate.

in diameter (Fig. 10(c)). It is obvious that the formed fractured agglomerate was composed of many tactoid-like regions in which the nanolayers were normal to the direction of the main crack propagation. They prevented the main crack from propagating straightly and resulted in the crack bifurcation. It can be clearly observed that two large crack branches formed. One branch turned left and continued to progress, the other branch turned right and terminated in the matrix. In particular, three small branches also formed and were arrested in the agglomerate. Subsequently, the main crack continued to progress in the matrix (Fig. 10(b)) and then propagated into the organoclay agglomerate ca. 2 μm in diameter by the debonding of the nanolayers along the direction of the main crack propagation (Fig. 10(a)). The main crack next bifurcated and formed two crack branches when it met with the tactoid-like regions in which the nanolayers were perpendicular to the direction of the main crack propagation. The left branch continued to propagate into the matrix, while the right branch first propagated into the agglomerate and then further bifurcated and formed another two crack branches when it met with the tactoid-like regions in which the nanolayers were normal to the direction of the crack propagation. However, since the further formed left branch terminated at the very early stage of the crack bifurcation, the remaining right branch showed that only the crack deflection took place. Furthermore, the zigzag pattern of the crack in Fig. 10(e) indicates that more fracture energy is needed for the HNCs compared with that of the homogeneous PES/epoxy blend whose crack is commonly straighter. On balance, these phenomena demonstrate that the speculation shown in Fig. 9 is reasonable.

It can also be seen from Figs. 8 and 10 that the debonding and bridging of the nanolayers were commonly accompanied by the plastic deformation of the matrices around them. The formation of the marked plastic deformation is very likely to relate to the relatively high content of the resins between the ordered exfoliated nanolayers. Consequently, based on the above toughening mechanisms of the nanolayers, it can be presumed that their ordered structure led to the crack bifurcation and crack deflection, while
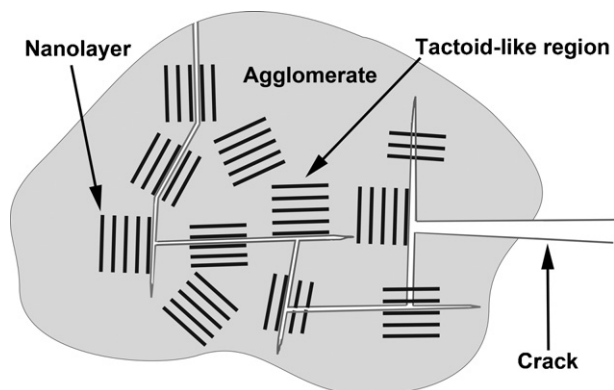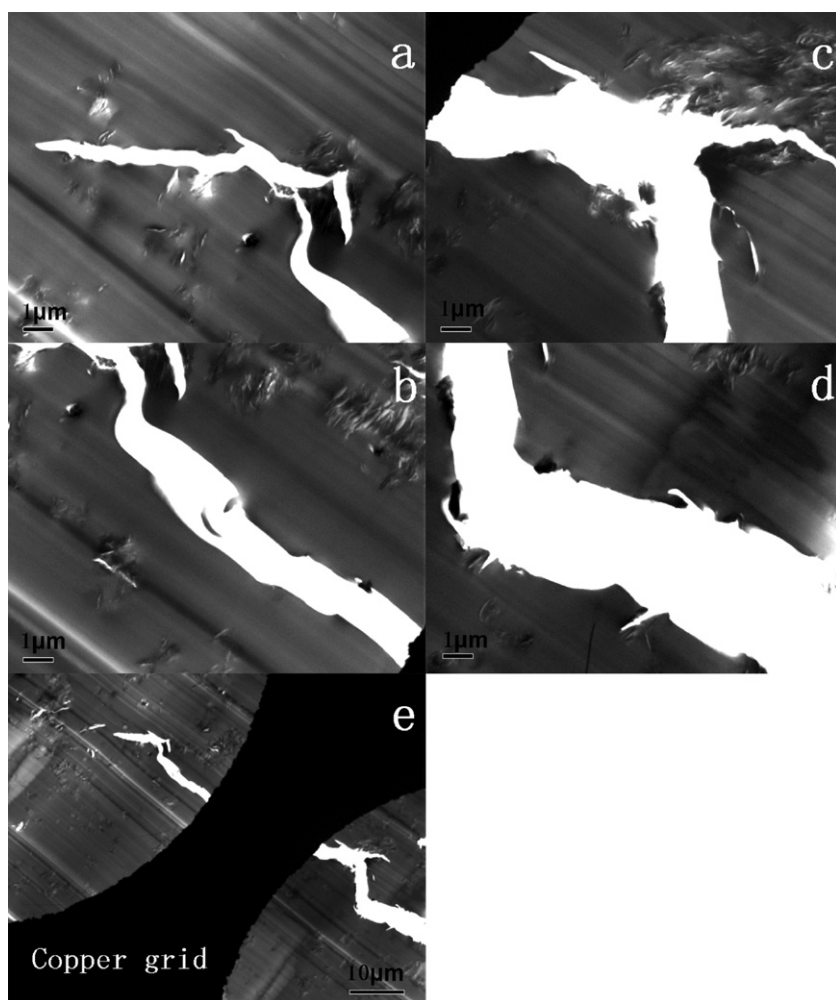
Fig. 10. Sub-critical crack in the HNC with 1 wt% organoclay acquired by DN-4PB technique: (a)–(d) are the close-ups of the four consecutive parts of the crack in (e). The crack was partially covered by the copper grid in (b), (c) and (e).

their exfoliated structure facilitated the large plastic deformation of the matrices.

Accordingly, the toughening mechanisms of the organoclay agglomerates are relative to those of the nanolayers. The debonding, bridging, various orientations of the nanolayers (Fig. 10) and the plastic deformations of the matrices they induced led to the crack front bowing (Fig. 5), crack bridging (Fig. 6), formation of the organoclay agglomerates with various fracture positions (Fig. 6) and debonding of the organoclay agglomerates from the matrices (Fig. 7). As a result, the present study shows that the toughening mechanisms of the HNCs on the micron-scale are strongly related to those on the nanoscale. The effective micron-scale toughening effects were attained through the nanoscale toughening effects, while the nanoscale toughening effects were more effective in the formed micron-scale regions. Since the crack bifurcation, crack deflection and deformation of the matrix generally took place to a large extent at the agglomerates over 1 μm in diameter (Fig. 10), we would like to term the organoclay agglomerate over 1 μm in diameter as organoclay-rich region and term the homogeneous PES/epoxy matrix as resin-rich region in this study. It is obvious that the degree of order and the orientations of the nanolayers in the organoclay-rich regions and the dimensions, the distribution and the content of the organoclay-rich regions are critical to the fracture toughness of the HNCs. Although it was hard for the nanolayers with small aspect ratio to induce the crack bifurcation, crack deflection and deformation of the matrices in the fully exfoliated nanocomposites [20], to form organoclay-rich regions composed of the tactoid-like regions with special orientations is expected to attain them. Therefore, the same or even lower fracture toughness of the fully exfoliated nanocomposites compared with that of the neat epoxy resin [13] is very likely to result from the absence of the micron-scale organoclay-rich region and the ordered structure.

4. Conclusions

HNCs with homogeneous PES/epoxy matrices and micron-scale organoclay agglomerates comprised of ordered exfoliated nanolayers were successfully prepared. The synergistic toughening effect of the organoclay and PES on epoxy resin was achieved. Their toughening mechanisms were described on the micron-scale and on the nanoscale, respectively. The incorporation of the PES into epoxy resin improved the ductility of the epoxy resin. The organoclay agglomerates induced crack front bowing, crack bridging, crack deflection, crack bifurcation and plastic deformation of matrices. The organoclay nanolayers with various orientations debonded from the matrices, bridged the cracks, and induced the plastic deformation of the matrices around them. This study shows that the toughening mechanisms of the micron-scale agglomerates and those of the nanolayers are correlative.

References

[1] J.H. Hodgkin, G.P. Simon, R.J. Varley, Polym. Adv. Technol. 9 (1998) 3–10.
[2] J. Lee, A.F. Yee, Polym. Eng. Sci. 40 (2000) 2457–2470.
[3] J. Frohlich, R. Thomann, O. Gryshchuk, J. Karger-Kocsis, R. Mulhaupt, J. Appl. Polym. Sci. 92 (2004) 3088–3096.
[4] C.B. Bucknall, H.G. Adrian, Polymer 30 (1989) 213–217.
[5] M.A. Andres, J. Garmendia, A. Valea, A. Eceiza, I. Mondragon, J. Appl. Polym. Sci. 69 (1998) 183–191.
[6] E.T. Thostenson, C. Li, T. Chou, Compos. Sci. Technol. 65 (2005) 491–516.
[7] M. Alexandre, P. Dubois, Mater. Sci. Eng. 28 (2000) 1–63.
[8] W. Liu, S.V. Hoa, M. Pugh, Compos. Sci. Technol. 65 (2005) 307–316.
[9] J.H. Park, S.C. Jana, Polymer 44 (2003) 2091–2100.
[10] A. Asif, K. Leena, V.L. Rao, K.N. Ninan, J. Appl. Polym. Sci. 106 (2007) 2936–2946.
[11] D. Ratna, O. Becker, R. Krishnamurthy, G.P. Simon, R.J. Varley, Polymer 44 (2003) 7449–7457.
[12] F.F. Lange, Philos. Mag. 22 (1970) 983–992.
[13] W.J. Boo, L. Sun, J. Liu, E. Moghbelli, A. Clearfield, H.J. Sue, H. Pham, N. Verghese, J. Polym. Sci. Part B: Polym. Phys. 45 (2007) 1459–1469.
[14] L.S. Sigl, Acta Mater. 44 (1996) 3599–3609.
[15] H. Kishi, Y.-B. Shi, J. Huang, A.F. Yee, J. Mater. Sci. 32 (1997) 761–771.
[16] B.J. Cardwell, A.F. Yee, J. Mater. Sci. 33 (1998) 5473–5484.
[17] J. Lee, A.F. Yee, Polymer 42 (2001) 589–597.
[18] H.J. Sue, Polym. Eng. Sci. 31 (1991) 275–288.
[19] J.F. Timmerman, B.S. Hayes, J.C. Seferis, Compos. Sci. Technol. 62 (2002) 1249–1258.
[20] W.J. Boo, L. Sun, G.L. Warren, E. Moghbelli, H. Pham, A. Clearfield, H.J. Sue, Polymer 48 (2007) 1075–1082.